Experimental Electron Density of the Ozonide ion (O_3^-) in Potassium Ozonide, KO_3

Thomas Kellersohn, Nikolaus Korber, and Martin Jansen*

Contribution from the Institut für Anorganische Chemie der Rheinischen Friedrich-Wilhelms-Universität, Gerhard Domagk Strasse 1, D-53121 Bonn, Germany

Received April 5, 1993®

Abstract: The deformation electron density in potassium ozonide has been determined by multipole refinement with the Hirshfeld formalism using single-crystal X-ray data collected at 170 K. No electron excess is observed in the oxygen–oxygen bond regions of the ozonide ion, a feature that is at first sight surprising, but it is not unusual for bonds between electronegative atoms. The explanation is that oxygen has a degenerate ground state with an open p shell, and therefore the total deformation density results from both chemical bonding effects and the superposition of nonspherical ground states. The former effect, if small, cannot compensate for the latter, and a net charge depletion results. The oxygen lone-pair regions exhibit well-distinguished maxima, while a charge depletion is found near O(2) in the direction of the shortest intermolecular O–O distances. This can be taken as an indication for a small electrostatic interaction between the paramagnetic ozonide anions, although the roles of "donor" and "acceptor" seem to be interchanged compared to the expectation from the relative polarities. On the basis of the refinement results, the terminal oxygen atoms carry more negative partial charge compared to the central atom, which is in agreement with quantum chemical calculations.

Introduction

The ozonide ion is of considerable general interest for the understanding of chemical bonding. It constitutes the simplest homonuclear, triatomic, paramagnetic 19-valence-electron system. Although it has been known to exist for a long time,[1,2] it is still regarded as a rather exotic species due to its very high reactivity. It was not possible until recently to determine its true physical properties, such as molecular geometry, because there was no viable synthetic route to pure samples. This is at least partly due to the fact that solid ionic ozonides are thermodynamically metastable and extremely sensitive to moisture and carbon dioxide. With use of a recently developed preparative method,[3] pure alkali metal ozonides can now be prepared in sufficiently large amounts for more detailed investigations and for use as starting material for additional syntheses.

About ten solid ozonides have been prepared up to now and their crystal structures were determined. Apart from the potassium, rubidium, and cesium compounds, other ozonides with various tetraalkylammonium cations[4] and alkali metal–crown ether complex cations[5] are sufficiently stable to have their structures characterized. In the present context, it is important to note that only KO_3 and RbO_3 exhibit indications of antiferromagnetic spin pairing of the ozonide ions below 10 K.[6] At the same time, the shortest *inter*molecular distances for ozonide ions are found in KO_3 and RbO_3, and the ozonide ion in KO_3 has the longest intramolecular O–O distance as well as the smallest *intra*molecular O–O–O angle in the whole series. This leads to the assumption that some intermolecular interactions are probably present in KO_3.

The formal bond order in the ozonide ion is 1.25, considerably less than that in the dioxygen cation (O_2^+, 2.5), the oxygen molecule (O_2, 2.0), the hyperoxide anion (HO_2^-, 1.5), and the ozone molecule (O_3, 1.5), but it is larger than that in the peroxide anion (O_2^{2-}, 1.0). A MO treatment[7] reveals that the 19th electron of the ozonide ion occupies the $2b_1$ antibonding molecular orbital. From naive population analyses (see also Figure 1) it can be inferred that the negative charge should mainly be accumulated on the terminal oxygen atoms, whereas the central oxygen atom should have a more positive partial charge. The arrangement of the ozonide ions in the structure of KO_3 confirms this; the shortest intermolecular O–O contacts are indeed found between the central O(1) and the terminal O(2) atoms of neighboring ozonide ions.

In contrast to innumerable quantum chemical studies which have been devoted to the ozone molecule during the last two decades, only three reports are concerned with the ozonide anion.[8] This is most probably due to the difficulties that are encountered when negatively charged species are treated with *ab initio* calculations. Nevertheless, the most recent calculations[9] show a good agreement of the calculated properties with the experimental values, such as bond length and angle, as well as electronic transition energies. However, no calculated electron density distribution has hitherto been reported. The questions to be answered on the basis of an experimental electron density study are the following: How are the electrons distributed within the ozonide ion? Can the different partial charges of the central and terminal oxygen atoms be distinguished in the electron density maps? Are the intermolecular interactions electrostatic in nature and, if so, can they be recognized from a polarization of the lone pairs?

Experimental Section

Synthesis and Crystal Growth. KO_3 was prepared by the reaction of solid potassium hyperoxide, KO_2,[10] with a gaseous oxygen/ozone mixture (*ca.* 5% ozone) obtained from a commercial ozone generator. The

* To whom correspondence should be addressed.

® Abstract published in *Advance ACS Abstracts*, October 15, 1993.

(1) For a review of results until the 1960's, see: (a) Vannerberg, N. G. *Prog. Inorg. Chem.* **1962**, 4, 125–197. (b) Vol'nov, I. I., *Peroxides, Superoxides, and Ozonides of Alkali and Alkaline Earth Metals*; Petrocelli, A. W., Ed.; Plenum Press: New York, 1966; pp 125–141.

(2) A review covering more recent results until 1988 is given by: Hesse, W.; Jansen, M.; Schnick, W. *Prog. Solid State Chem.* **1989**, *19*, 47–110.

(3) Schnick, W.; Jansen, M. *Angew. Chem.* **1985**, *97*, 48–49; *Angew. Chem., Int. Ed. Engl.* 1985, *24*, 56–57.

(4) Hesse, W.; Jansen, M. *Angew. Chem.* **1988**, *100*, 1388–1389; *Angew. Chem., Int. Ed. Engl.* 1988, *27*, 1341–1342.

(5) (a) Korber, N.; Jansen, M. *J. Chem. Soc., Chem. Commun.* 1990, 1654–1655. (b) Korber, N.; Jansen, M. *J. Am. Chem. Soc.*, accepted for publication. See also: (c) Korber, N. Ph.D. Thesis, University of Bonn, 1992.

(6) Lueken, H.; Deussen, M.; Jansen, M.; Hesse, W.; Schnick, W. *Z. Anorg. Allg. Chem.* **1987**, *553*, 179–186.

(7) Cremer, D. *The Chemistry of Functional Groups, Peroxides*; Patai, S., Ed.; John Wiley & Sons Ltd.: New York, 1983; pp 1–84.

(8) (a) Heaton, M. M.; Pipano, A.; Kaufman, J. J. *Int. J. Quantum Chem., Quantum Chem. Symp.* **1972**, *6*, 181–186. (b) Ohta, K.; Nakatsuiji, H.; Hirao, K.; Yonetzawa, T. J. *Chem. Phys.* **1980**, *73*, 1770–1776. (c) Peterson, K. A.; Mayrhofer, R. C.; Woods, R. C. *J. Chem. Phys.* **1990**, *93*, 5020–5028.

(9) Koch, W.; Frenking, G.; Steffen, G.; Reinen, D.; Jansen, M.; Assenmacher, W. *J. Chem. Phys.* **1993**, *99*, 1271–1277.

(10) Helms, A.; Klemm, W. *Z. Anorg. Allg. Chem.* **1939**, *241*, 97–106.

0002-7863/93/1515-11254$04.00/0

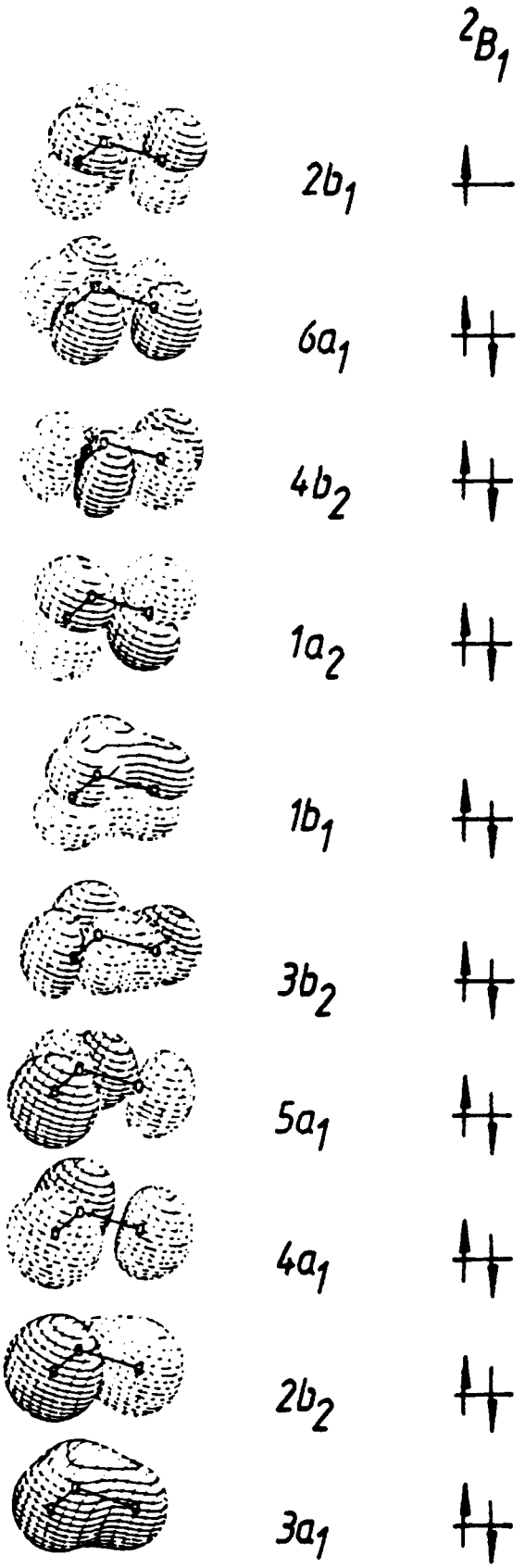

Figure 1. Sequence and approximate shape of the molecular orbitals for the free ozonide ion; contour plots are from ref 7 and the sequence of MO's follows that given in ref 9.

formation of the ozonide is exothermic, but it needs a sufficient activation energy for the first step, i.e. the cleavage of ozone into oxygen atoms and O_2 molecules on the surface of the hyperoxide. Competitively, the decomposition of the ozonide begins slightly above room temperature; therefore, an optimized temperature program during the reaction is essential. The reaction was accomplished in a specially designed apparatus[11] which allows controlled cooling (25 → −70 °C within 1 h) of the reaction zone during the synthesis as well as a subsequent extraction of the soluble ozonide from the remaining insoluble hyperoxide with liquid ammonia. In order to purify the crude potassium ozonide, it was recrystallized from liquid ammonia. The growth of single crystals suitable for the diffraction experiment was accomplished by slow evaporation of the ammonia at −50 °C. Crystals were selected and sealed in glass capillary tubes under argon and, after repeated shock-cooling in liquid nitrogen, quickly transferred to the cold stream of the diffractometer.

Table I. Crystallographic Data for KO_3

M_r	87.097
cryst system	tetragonal
space group	$I4/mcm$[a]
a, pm	862.31(13)
c, pm	712.79(11)
V, nm^3	0.53001(11)
D_x, Mg·m^{-3}	2.183
T, K	170(5)
Z	8
λ(Mo Kα), Å	0.71073
μ, cm^{-1}	16.17
$F(000)$	344
no. of measd reflcns	7759 (excl standards)
R(internal) (all data)	0.0220
$R(F^2)$	0.0189
$wR(F^2)$	0.0227
no. of unique reflcns	703
no. of reflcns considered obsd [$I \geq 2\sigma(I)$]	411
no. of refined parameters	65
extinction corr	insignificant
goodness-of-fit, S	1.11
δR plot: slope s	1.08
y intercept	−0.12
reflcns with $\Delta/\sigma \geq 4.0$	3

[a] No. 140 in ref 24.

X-ray Data Collection. A monocapped rectangular prismatic crystal was used with boundary planes (100), ($\bar{1}$00), (010), (0$\bar{1}$0), (001), (011), and (0$\bar{1}$1), size 0.331 × 0.188 × 0.165 mm, and volume 1.23 × 10^{-2} mm^3. The intensity measurement was performed on an Enraf-Nonius CAD4 diffractometer equipped with a nitrogen stream cooling device. The temperature was kept at 170 (±1) K with an estimated absolute inaccuracy of ±5 K. At lower temperatures, the long-term stability of the instrument became a problem. Graphite (002) monochromatized Mo Kα radiation was used. The cell dimensions were determined by a least-squares fit of the setting angles of 25 well-centered reflections in the range 34° < 2θ < 46°. ω–2θ scans were made with $\Delta\omega = (0.80 + 0.35 \tan\theta)°$ and a maximum measuring time of 300 s per reflection. Up to $2\theta = 30°$, a full sphere of reflections was measured ($-12 \leq (h,k) \leq 12$, $-10 \leq l \leq 10$), while only a hemisphere of reflections was measured between $2\theta = 30°$ and $2\theta_{max} = 100°$, $[(\sin\theta)/\lambda]_{max} = 1.09$ Å^{-1}, $-18 \leq (h,k) \leq 18$, $0 \leq l \leq 15$. The intensities of four reference reflections, measured every 60 min, decreased uniformly by 19.5% during the 496 h of data collection due to irradiation damage of the crystal. Despite this considerable decay, a linear correction proved to be adequate. The background correction was performed according to the procedure given by Lehmann and Larsen.[12]

An absorption correction by Gaussian integration was applied (transmission range 0.586–0.766). An empirical absorption correction based on the ψ-scan intensities of 10 reflections was performed for comparison and gave essentially the same result. Crystallographic data and further details are given in Table I.

Refinements. The full-matrix least-squares program DUPALS was used for the refinements.[13] The atomic positions from a conventional refinement of 250 K X-ray data[14] were taken as starting values. Extinction effects were found to be neglegible, most probably due to the repeated shock-cooling of the crystal in liquid nitrogen before the data collection.

To minimize the effects of experimental noise, which is inevitably present in X–$X_{high\ order}$ or X–N Fourier syntheses, modeling of the electron deformation density by multipole fitting is generally to be preferred. This

(11) Schnick, W.; Jansen, M. *Z. Anorg. Allg. Chem.* **1986**, *532*, 37–46.
(12) Lehmann, M. S.; Larsen, F. K. *Acta Crystallogr.* **1974**, *A30*, 580–584.
(13) Lundgren, J. O. *Crystallographic Computer Programs*, Report UUIC-B13-04-05, 1982. Institute of Chemistry, University of Uppsala, Sweden.
(14) Schnick, W.; Jansen, M. *Rev. Chim. Mineral.* **1987**, *24*, 446–456.

Table II. Fractional Atomic Coordinates and Anisotropic Displacement Parameters $U_{ij}/10^{-2}$ Å^2 for KO_3 Based on the Multipole Refinement of the 170 K Data

atom	Wyckoff site	x	y	z	U_{11}	U_{22}	U_{33}	U_{12}	U_{13}	U_{23}
K(1)	4a	0.0	0.0	0.25	1.99(3)	U11	1.66(4)	0.0	0.0	0.0
K(2)	4b	0.0	0.5	0.25	2.49(2)	U11	1.73(4)	0.0	0.0	0.0
O(1)	8h	0.28053(19)	0.21947(19)	0.0	2.07(4)	U11	6.32(17)	0.10(4)	0.0	0.0
O(2)	16k	0.24908(13)	0.06672(17)	0.0	2.05(3)	2.24(4)	2.95(5)	−0.54(3)	0.0	0.0

is also true for centrosymmetric structures, where phase errors do not distort the deformation electron density maps as severely as they do for noncentrosymmetric structures. We employed the multipole deformation functions proposed by Hirshfeld[15] with modifications by Harel and Hirshfeld[16] and Hirshfeld.[17] The spherical charge density at each atomic site is modified by an expansion of up to 35 terms with the general form

$$\rho_n(r,\theta_k) = N_n r^n \cos^n \theta_k \exp(-\gamma r^2)$$

centered on the site, where r and θ_k are polar coordinates in the kth of a chosen set of axes, n and k are integers [$n = 1, 2, 3, 4$; $k = 1,\ldots, (n+1)(n+2)/2$], and N_n are normalization factors. The scattering factor for each atom is then

$$f_l = f_{spher,l} + \sum C_l \varphi_l$$

where φ_l are the Fourier transforms of the expansion of the deformation density. The (population) parameters C_l are refineable.

A series of deformation refinements was performed, where initially imposed symmetry constraints, as e.g. cylindrical symmetry on O(2), were successively relaxed, and the level of n was raised. The significance of each increase in sophistication of the model was checked by inspection of the goodness of fit and the δR plot.[18] It was observed during this series that the δR plots changed their shape drastically from sigmoidal to nearly linear, which is a very good indicator that the model is increasingly accurate. In the final set, one scale factor and the following parameters were refined: K(1), $n \leq 4$, site symmetry 422, $\gamma = 3.5$, β_{ij} and 7 deformation parameters; K(2), $n \leq 4$, site symmetry $42m$, $\gamma = 3.5$, β_{ij} and 7 deformation parameters; O(1), $n \leq 4$, site symmetry $mm2$, $\gamma = 3.5$, x, β_{ij} and 14 deformation parameters; and O(2), $n \leq 4$, site symmetry m, $\gamma = 3.5$, x, y, β_{ij} and 22 deformation parameters.

The quantity minimized was $\sum w(|F_o|^2 - |F_c|^2)^2$, where $w^{-1} = \sigma^2_{count}|F_o|^2 + k^2|F_o|^4$. The refinements were considered to be converged when $\Delta/\sigma \leq 0.001$. For comparison, $R(F^2)$ is 0.0782 for all 703 unique reflections with $(\sin\theta)/\lambda \leq 1.09$. The refinement of the conventional (spherical) model converged at $R(F^2) = 0.0267$, $wR(F^2) = 0.0343$. The deformation refinement thus gave a significant improvement (see Table I).

After the refinements, the model deformation density was calculated as a Fourier summation over a full set of independent structure factors up to $(\sin\theta)/\lambda = 1.09$. These structure factors were calculated by setting all spherical atomic scattering factors and the thermal parameters to zero. Therefore the model deformation density maps are so-called "static maps" which exclude the effects of thermal motion, but they are not free of series-termination errors.

Results and Discussion

General features of the structure have already been described.[3,14] Figure 2 shows the atomic arrangement in KO_3. Atomic coordinates and anisotropic displacement parameters are given in Table II and interatomic distances and angles in Table III. The planes in which the electron density has been calculated are depicted in Figure 3. The atomic coordinates agree with the results of the conventional refinement of X-ray data collected at 250 K[14] within their combined esd's. The effect of the lower temperature in the present study shows up in the slightly smaller lattice constants and the smaller displacement parameters. The anisotropy of the O(1) displacement parameters is still observable but less pronounced than that in the previous study. This is most probably due to the fact that the central O(1) interacts much less with the K^+ cations than does the terminal O(2). A coarse extrapolation of the displacement parameters down to 0 K leaves no significant residual, indicating that there is no statistical disorder present. However, for the K^+ ions anharmonic thermal motion effects cannot be excluded reliably. Therefore, the K^+ deformation density maps are not considered further. This does not affect the results and discussion for the ozonide ion.

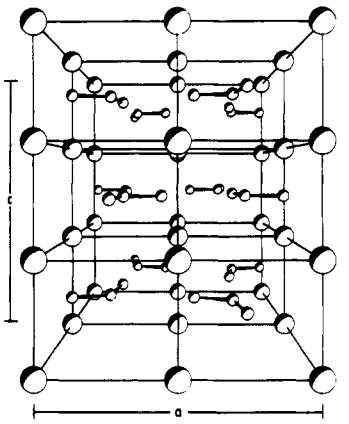

Figure 2. Structure of KO_3; projection of the unit cell.

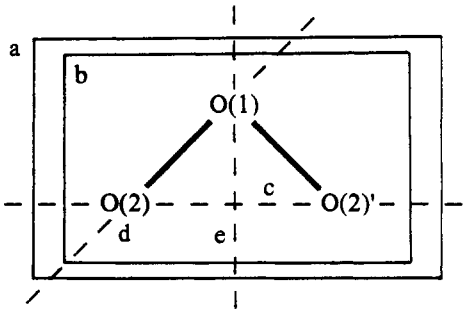

Figure 3. Positions of the sections displayed in Figure 4. Vertical planes are represented by dashed lines.

Table III. Interatomic Distances (pm) and Angles (deg) for KO_3 Based on the Multipole Refinement of the 170 K Data; Distances up to 360 pm Are Considered

	Ozonide Ion	
O(1)–O(2)	134.5(2)	2×
O(2)–O(2)	224.6(3)	1× (intramolecular)
O(2)–O(1)–O(2)	113.3(1)	1×
	Shortest Intermolecular O···O Distances	
O(1)···O(2)	300.5(2)	2×
O(2)···O(2)	314.5(2)	2×
	Potassium–Oxygen Distances	
K(1)–O(2)	284.9(1)	8×
K(1)–O(1)	355.1(1)	8×
K(2)–O(2)	286.2(1)	8×
K(2)–O(1)	321.5(1)	8×

Deformation Electron Densities. The most striking feature of the deformation electron density map in the O(2)–O(1)–O(2) plane is the absence of electron accumulation in the O–O bonds, see Figure 4a. At first sight, this seems to be surprising and contrary to many studies where an electron excess in covalent bonds has almost always been observed. However, an X–N electron density study on hydrogen peroxide[19] has revealed a similar apparent charge depletion in the O–O bond, and another independent observation of this effect has been made in an X–X

(15) Hirshfeld, F. L. *Acta Crystallogr.* **1971**, *B27*, 769–781.
(16) Harel, M.; Hirshfeld, F. L. *Chem. Scr.* **1975**, *26*, 389–394.
(17) Hirshfeld, F. L. *Isr. J. Chem.* **1977**, *26*, 226–229.
(18) Abrahams, S. C.; Keve, *E.T. Acta Crystallogr.* **1971**, *A27*, 157–165.

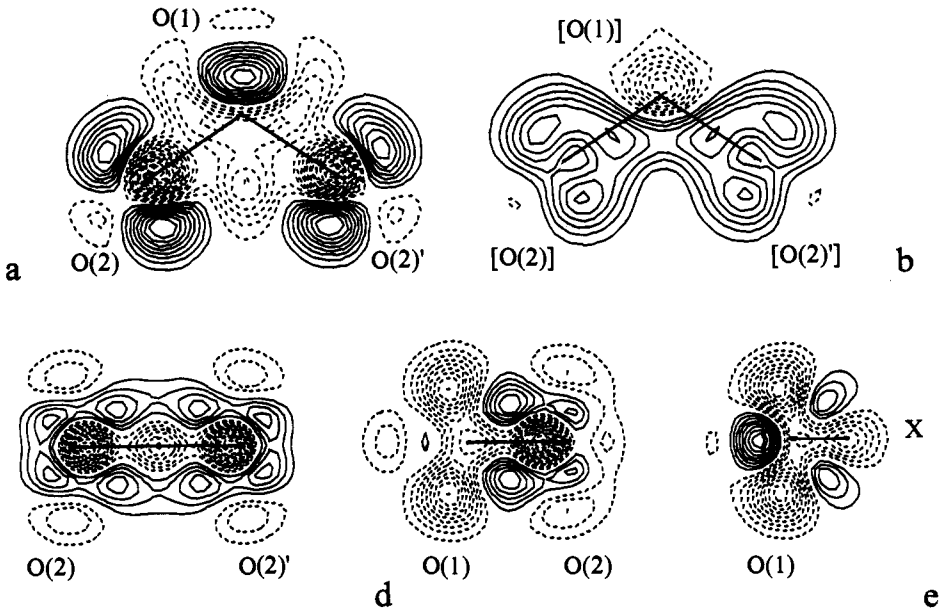

Figure 4. Static model deformation density of the ozonide ion: (a) O–O–O plane; (b) plane parallel to (a) at a distance of 0.5 Å; (c) plane perpendicular to (a) containing the two O(2) atoms; (d) plane perpendicular to (a) containing the O(1)–O(2) bond; and (e) plane perpendicular to (a) containing the bisector of the O(2)–O(1)–O(2)′ angles, where "×" denotes the point between O(2) and O(2)′. Contour intervals at 0.05 e·Å^{-3}, negative contours (electron deficiency) are dashed, positive contours (electron excess) are drawn as full lines, zero contour is omitted. Atomic positions close to the displayed planes are labeled in brackets.

study on 1,2,7,8-tetraaza-4,5,10,11-tetraoxatricyclo[6.4.1.1^{2,7}]-tetradecane.[20]

What is the reason for the charge depletion in such bonds? An explanation has been proposed by Schwarz *et al.*[21] All observed deformation densities depend, of course, on the reference system which is chosen. The deformation electron densities which we consider here represent the charge redistribution in the molecule in question relative to a promolecule which is constructed from noninteracting, spherical averaged ground-state atoms. Such deformation densities have been called "total deformation densities". However, atoms having degenerate electronic ground states, such as oxygen, are *not* spherical. The observed total deformation density is thus a superposition of genuine chemical bonding effects and the effect of nonspherical ground states. It seems difficult to include the asphericity of the constituent atoms in a least-squares deformation density refinement program, since both the orientation and the orbital populations of the prepared valence-state atoms must be optimized and cannot be determined *a priori*. Nevertheless, early results of such efforts have recently been reported.[22]

Against this background, the aforementioned apparent charge depletion in the oxygen–oxygen bond can be quite well understood, and it even corresponds to our expectations. Even the relative magnitude of this depletion can be correlated with the formal bond order as introduced above—as far as such a trend can reasonably be deduced on the basis of the limited number of comparable studies.

The plane 0.5 Å above the O–O–O plane (Figure 4b) shows an electron excess throughout, which can be taken as an indication of π-bonding. Figures 4c,d,e give complementary sections of interest. Surprisingly, the deformation density does not vanish between the two O(2) atoms, although one cannot postulate a real chemical bond between them.

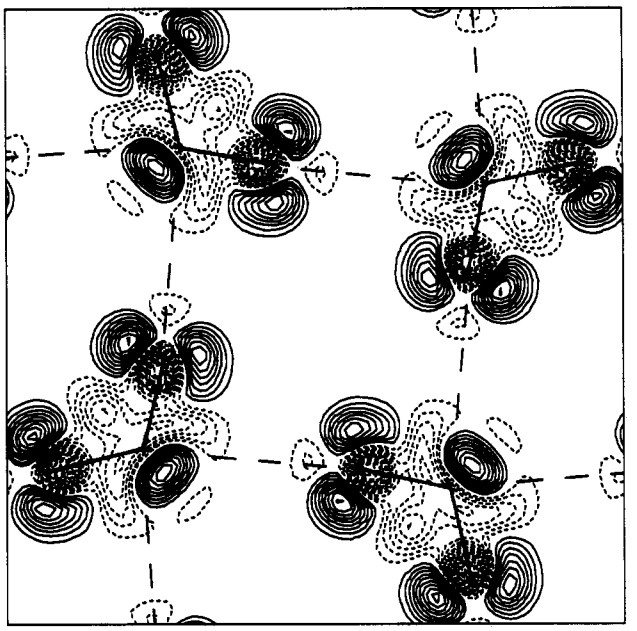

Figure 5. Section of the unit cell of KO_3 in the plane (x, y, 0.0) showing the mutual arrangement of four ozonide ions. The shortest intermolecular O(1)···O(2) distances are represented as dashed lines. The edges of the box correspond to a and b, respectively. For more explanations, see Figure 4.

In the oxygen lone-pair region, genuine chemical bonding effects and the ground-state asphericity act in the same direction and lead to well-pronounced maxima in the experimental maps (see Figures 4a and 5). Although the observed maxima are therefore too high, their spatial arrangement should not be falsified by this effect. From a section of the unit cell containing four (coplanar) ozonide ions it becomes obvious that the lone-pair maxima of O(2) in the molecular plane avoid being directed along the shortest intermolecular O(1)···O(2) distances, see Figure 5. We suggest, therefore, that weak electrostatic interactions are indeed present.

Another indication of intermolecular interaction is given by the partial charges of the oxygen atoms which can be deduced from the refined multipole model using the Hirshfeld partitioning

(19) Savariault, J. M.; Lehmann, M. S. *J. Am. Chem. Soc.* **1980**, *102*, 1298–1303.

(20) Dunitz, J. D.; Seiler, P. *J. Am. Chem. Soc.* **1983**, *105*, 7056–3058.

(21) (a) Schwarz, W. H. E.; Reudenberg, K.; Mensching, L. *J. Am. Chem. Soc.* **1989**, *111*, 6926–6933. (b) Mensching, L.; Von Niessen, W.; Valtazanos, P.; Ruedenberg, K.; Schwarz, W. H. E. *J. Am. Chem. Soc.* **1989**, *111*, 6933–6941, see also references therein.

(22) Miller, L. L.; Schwarz, W. H. E.; Niu, J. E. *Proceedings of Sagamore X*; Springborg, M., Saenz, A., Weyrich, W., Eds.; Konstanz, Germany, 1991; p 84.

scheme. Although their absolute values are not reliable, since they depend strongly on the integration method, their relative order should be *qualitatively* correct. We find a partial charge of +1.2 e for O(1) and −1.0 e for each O(2). The terminal oxygen atoms thus carry more of the excess negative charge than the central one. This is in agreement with the geometric arrangement found in KO_3, with the population analysis of the molecular orbitals, and with the results of the most reliable *ab initio* calculations.[9]

However, the lone-pair peaks at O(2) do not lie on the O(1)···O-(2) line, while the lone-pair peak of O(1) does to some extent. The picture is therefore contrary to what is observed for electrostatic dipole–dipole interactions as *e.g.* in a hydrogen bond.[23] In the latter case, the lone-pair peaks of the hydrogen bond acceptor (usually oxygen), which is the negative part of the dipole, are polarized toward the region of electron deficiency at the proton of the hydrogen-bond donor. This effect seems to be reversed in the present case, since, based on the discussion above, one would expect O(2) to be an electron donor and O(1) to be an electron acceptor. However, the lone pairs at O(1) have less space available than those at O(2) and are forced to lie opposite the intramolecular O(1)–O(2) bonds. The observed electron density distribution seems to be the best possible compromise between the electrostatic attraction of different (partial) charges and the repulsion of regions with electron accumulation—the lone pairs.

(23) See, for instance: Feil, D. *J. Mol. Struct.* **1990**, *237*, 33–46.
(24) *International Tables for Crystallography*, Hahn, Th., Ed.; D. Reidel Publishing Co.: Dordrecht, The Netherlands, 1983; Vol. A.

Concluding Remarks

This study has demonstrated that electron density studies can be performed on markedly unstable compounds, provided that appropriate care is taken with the crystal growth and the diffraction experiment. Obviously, for a more quantitative assessment of the intermolecular electronic interactions of ozonide ions in the solid state, further studies employing this method are highly desirable. The tetraalkylammonium ozonides are especially interesting, since systematically shorter O–O bond distances and larger O–O–O bond angles have been observed. Such investigations are planned. More detailed quantum chemical studies are also desirable, since our experimental results invite comparison.

Acknowledgment. We thank Mr. K. Armbruster and Dipl.-Chem. W. Assenmacher for experimental assistance. Financial support has been provided by the Deutsche Forschungsgemeinschaft and the Fonds der Chemischen Industrie, which are gratefully acknowledged. Th.K. thanks the Deutsche Forschungsgemeinschaft for a post-doctoral scholarship.

Registry Numbers supplied by author: Potassium hyperoxide (KO_2), 12136-46-8; potassium ozonide (KO_3), 12030-89-6.

Supplementary Material Available: Tables of refined population parameters (2 pages); listing of observed and calculated structure factors (7 pages). Ordering information is given on any current masthead page.